Electronic Supplementary Material (ESI) for Nanoscale.

Supplementary Information

A Flexible Metallic Actuator Using Reduced Graphene Oxide as a Multifunctional Component

Junxing Meng,[a,1] Jiuke Mu,[a,1] Chengyi Hou,*[a] Qinghong Zhang,[b] Yaogang Li,[b] Hongzhi Wang*[a]

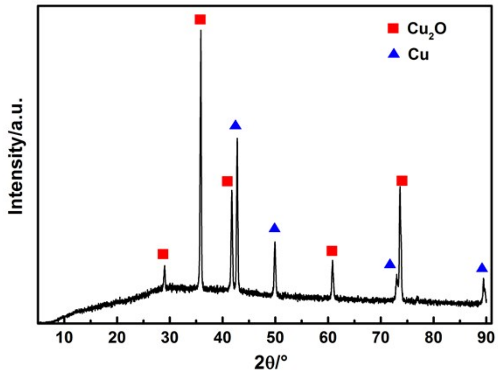

Figure S1. XRD patterns of oxide surface for the actuator with blue squares and red triangles showing the standard peaks of Cu_2O and Cu.

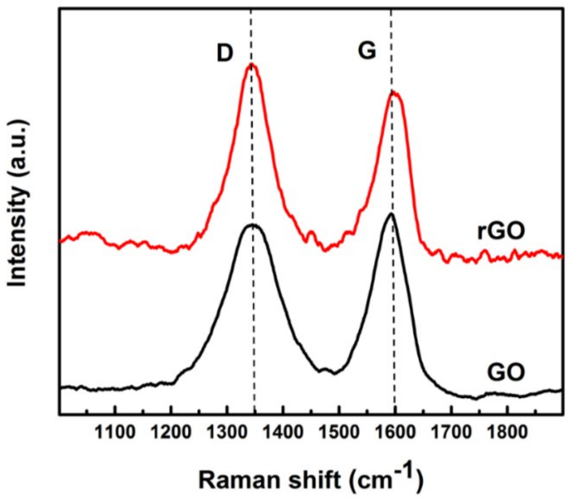

Figure S2. The upper curve shows the Raman shift of oxide face for the actuator, or in other words, the copper-contacted face of the GO gel (Fig. 1). The lower curve shows the Raman shift of GO gel (without contact to copper) used for fabricating the flexible actuator.

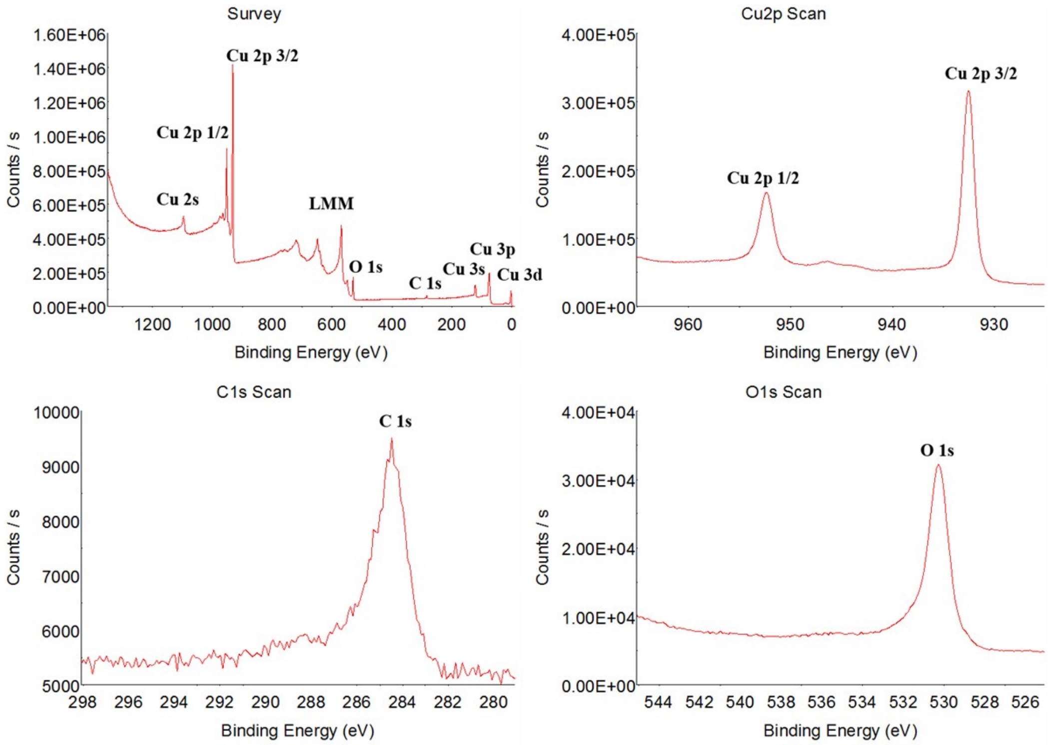

Figure S3. X-ray photoelectron spectroscopy of oxide face for the actuator.

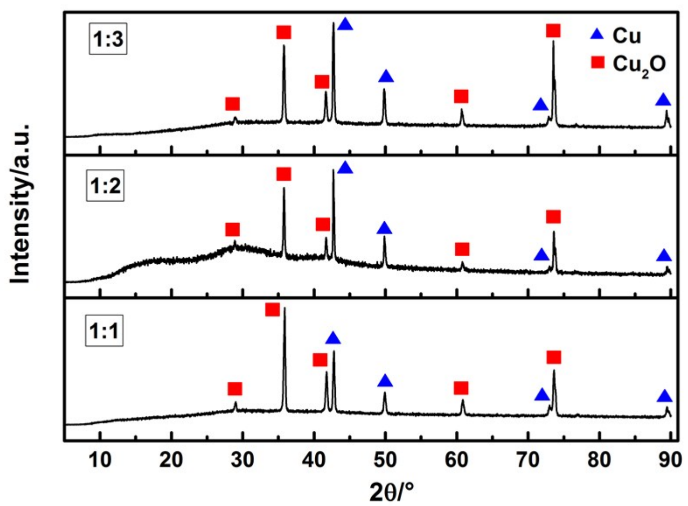

Figure S4. XRD patterns of oxide face for the actuator with different thickness ratios.

The blue squares and red triangles show the standard peaks for Cu and Cu_2O.

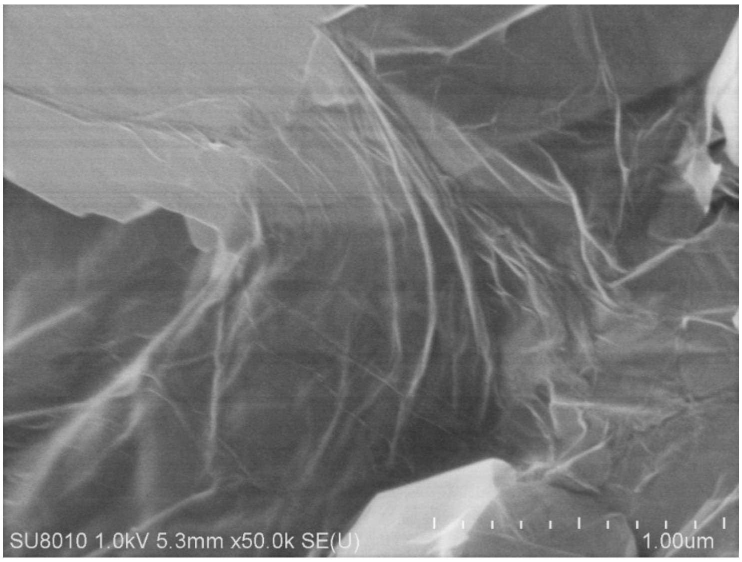

Figure S5. Surface FE-SEM images of the oxide face with rGO sheets attaching on the surface of Cu_2O particles.

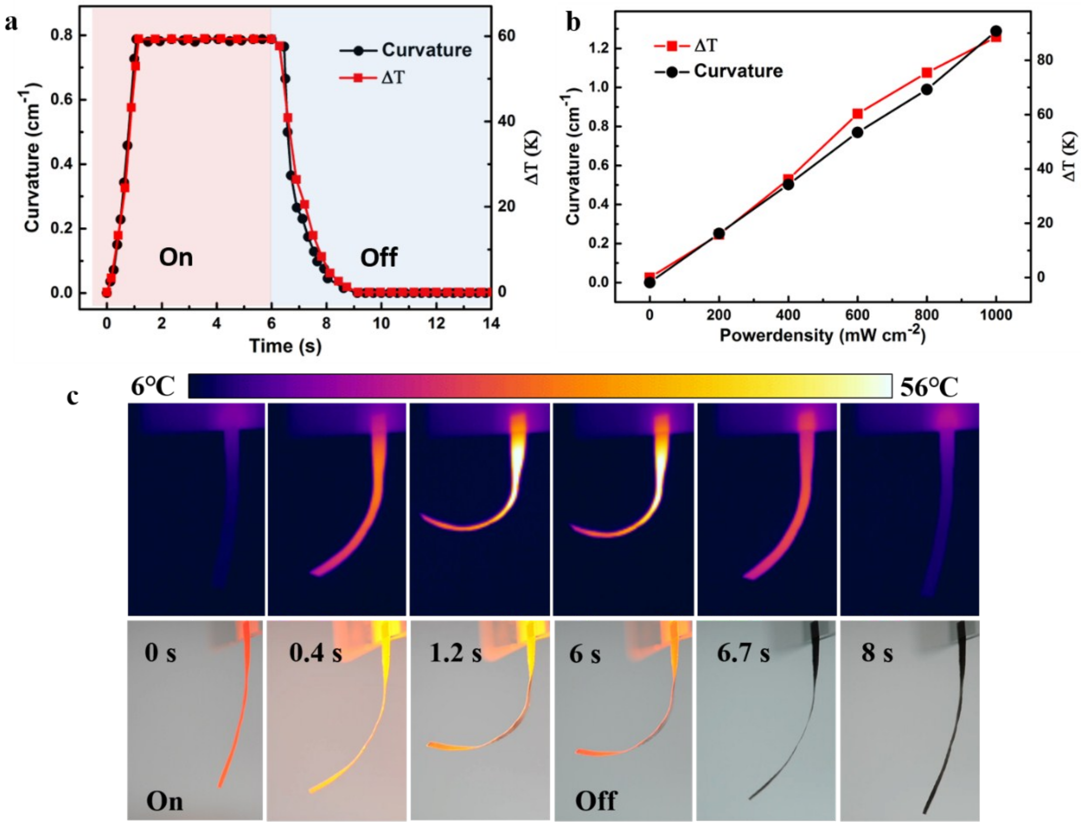

Figure S6. (A) The curvature and temperature variation as results of time for the actuator with infrared irradiation (600 mW cm^{-2}) on and off. When the actuator was exposed to infrared irradiation, the bending motion immediately happened with light on, and reached maximum curvature within 2 s. (B) The maximum curvature and temperature variation as results of power density for the actuator. Increasing power density of infrared irradiation leads to increasing maximum curvature. (C) Digital photos and thermal images of the actuator (4 cm x 4 mm) triggered by infrared irradiation. The emissivity was calibrated detailed in Supplementary Information (Figure S7 and Note S2). Directly heating was also studied by putting the actuator on a hot plate for direct contact heat exchange. The actuator was cut into Mimosa pudica inspired shape with leaf arrays on both side (see Movie 2). The high thermal conduction of the flexible actuator promised instantaneous deformation. Besides, the stable structure enables the actuator work well in water heated on hot plate, shown in Movie 3.

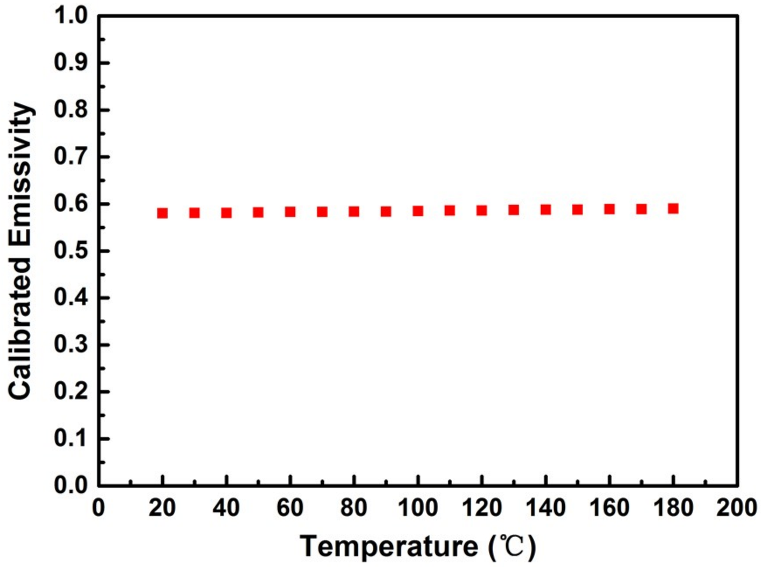

Figure S7. Calibrated emissivity of Cu_2O layer for the actuator as a function of temperature with nearly constant value of 0.585.

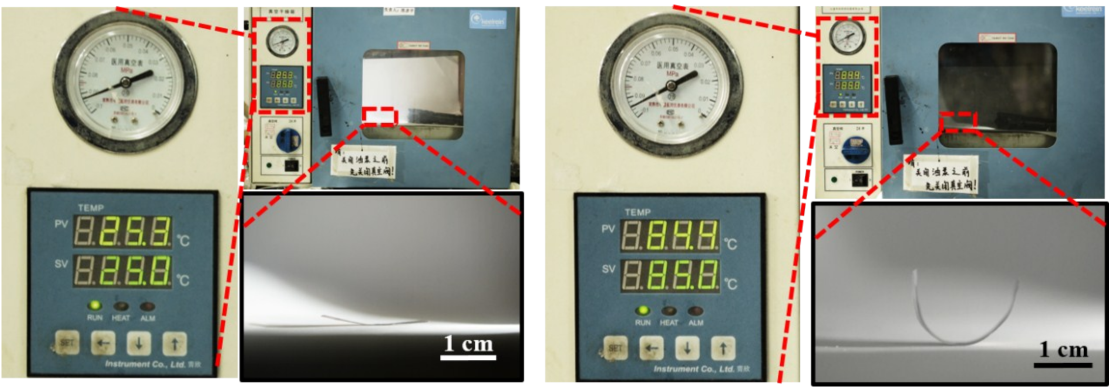

Figure S8. The thin film actuator is bending in vacuum (pressure ~ -94 KPa).

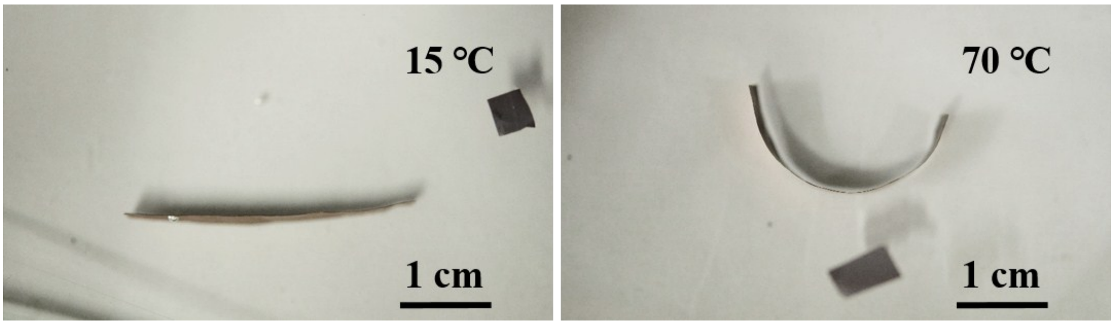

Figure S9. The thin film actuator is bending in water.

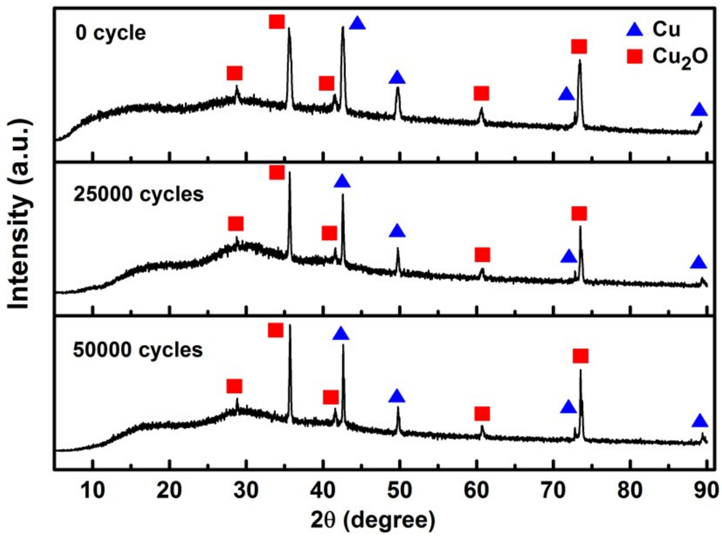

Figure S10. XRD patterns of oxide face for the actuator with cycles of 0, 25000 and 50000 times. The blue squares and red triangles show the standard peaks for Cu and Cu_2O.

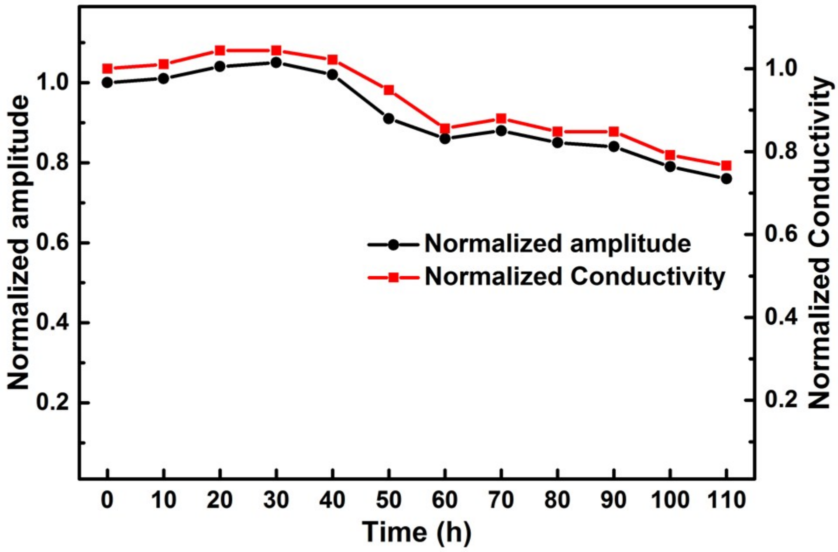

Figure S11. Reliability test under continuously applied voltage (1 V). The slightly reduced electric conductivity and amplitude were resulted from the deep oxidation of copper surface in humid air.

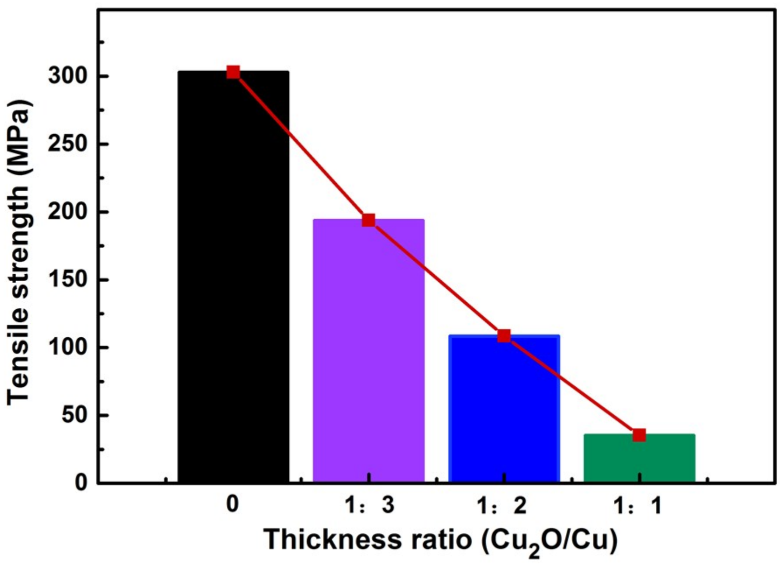

Figure S12. The tensile strength of the flexible actuator with different thickness ratios.

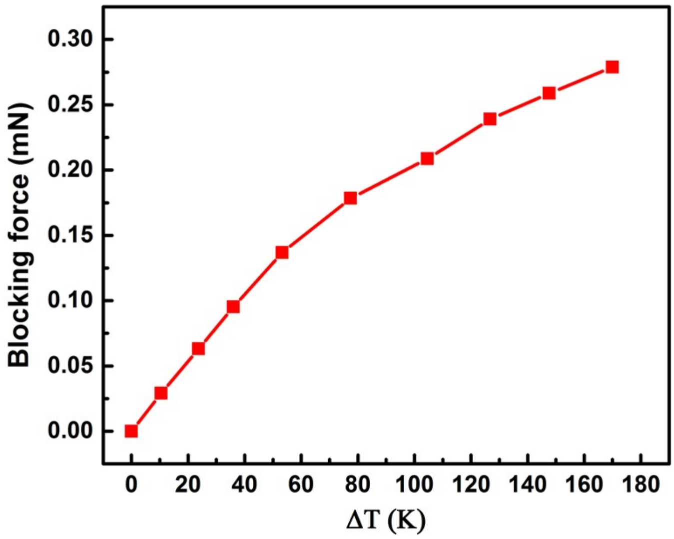

Figure S13. Blocking force of the flexible actuator as a function of temperature variation.

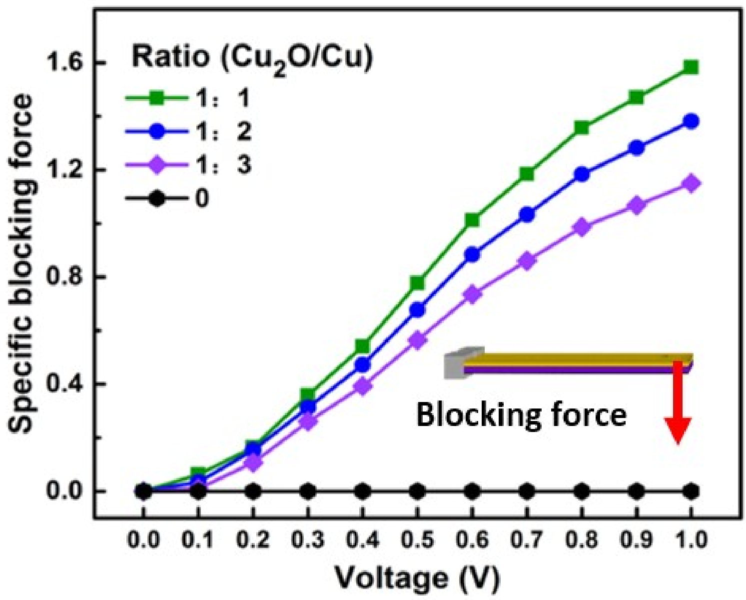

Figure S14: The specific blocking force as a function of applied voltage for the flexible actuator with different thickness ratios. The inset shows the measuring method of the vertical blocking force.

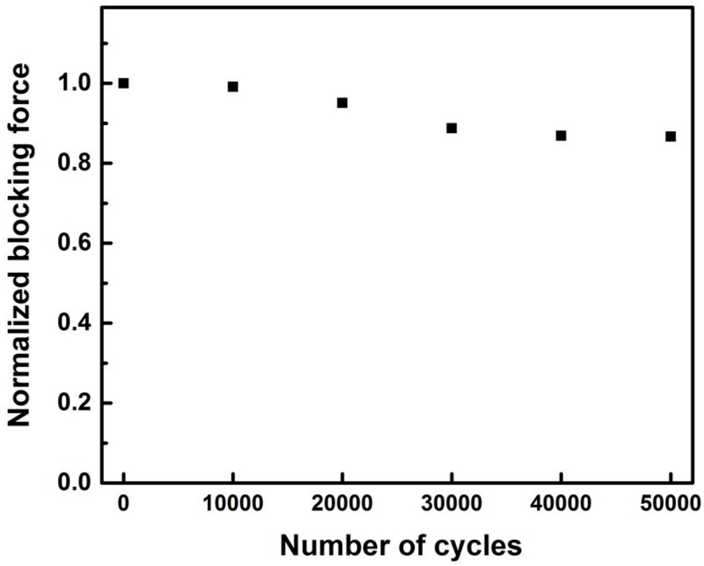

Figure S15: The reliability test of blocking force. Up to 50000 on/off cycles were performed under ambient laboratory conditions.

Note S1. Discussions on the redox reaction between copper and GO.

In the GO reduction experiments, the reductant (i.e., copper in our work) undergoes charge transfer interaction with function groups of GO. The reaction between GO and copper can be roughly written as:

$Cu - 2e^- \rightarrow Cu^{2+}$ (1)

$-OH + H^+ + e^- \rightarrow H_2O$ (2)

or

$Cu + 2{-OH} + 2H^+ \rightarrow Cu^{2+} + 2H_2O$ (3)

where H^+ comes from acidic systems, and $-OH$ represents a typical function group of GO.

But note that $-OH$ can not represent the full image of GO surface groups. Therefore, we should put GO and rGO in equation (2):

$GO + H^+ + e^- \rightarrow reduced\ GO + H_2O$ (4)

So, equation (3) can be written as:

$Cu + 2GO + 2H^+ \rightarrow Cu^{2+} + 2reduced\ GO + 2H_2O$ (5)

Note S2. Calibration of emissivity for Cu_2O layer

Because of the special structure of Cu_2O layer in this work, the emissivity was calibrated using carbon black as reference substance. Carbon black and the flexible actuator, with Cu_2O layer upward, were put adjacent to each other over the hot plate. The temperature of carbon black was recorded as known material with emissivity of 0.95, and the emissivity of the Cu_2O layer was adjusted until the obtained temperature matched the value of carbon black. The adjusted emissivity was used for Cu_2O layer with nearly constant value of 0.585, and the emissivity of Cu_2O layer was plotted as a function of temperature in Figure S7.

Note S3. Conversion efficiency of light to thermal power

When the flexible actuator is exposed to infrared light, the Cu_2O absorbs the photonic energy, which is converted into thermal energy. After reaching the saturating temperature, the heating power from infrared is balanced by radiation and convection with air. Similar to electric-heating system, the equation expressing the equilibrating state follows:[3]

$$P_i = P_c + P_r \tag{1}$$

$$P_c = hA(T_a - T_s) \tag{2}$$

$$P_r = \varepsilon\sigma A(T_a^4 - T_s^4) \tag{3}$$

where P_i is the total power loss of the actuator, P_c and P_r are the convective and radiative power loss of the actuator, h is the total convective heat-transfer coefficient of the actuator, A is the surface area, T_a is the temperature of the actuator, T_s is the temperature of the surrounding air, ε is the total emissivity of the actuator, and σ is the Stefan-Boltzmann constant. When the actuator achieves the balanced state, the temperature of the actuator stabilizes at a constant value, thus the total power loss of the actuator is approximately equal to the obtained power from infrared irradiation, where the conversion efficiency of the actuator can be expressed as:

$$\delta = \frac{P_i}{P_L} = \frac{hA(T_a - T_s) + \varepsilon\sigma A(T_a^4 - T_s^4)}{P_L} \tag{4}$$

where P_L is the infrared power density.

Note S4. Curvature of bimorph actuator

For a bimorph actuator composed of two layers with different material properties applied with temperature variation, the bending motion is due to the mismatch of the two layers with different thermal strain. The resulting curvature follows the Timoshenko' theory:[1]

$$k = \frac{1}{r} = \frac{6b_1b_2E_1E_2t_1t_2(t_1+t_2)(\propto_2 - \propto_1)\Delta T}{(b_1E_1t_1^2)^2 + (b_2E_2t_2^2)^2 + 2b_1b_2E_1E_2t_1t_2(2t_1^2 + 3t_1t_2 + 2t_2^2)} \quad (1)$$

where k is the curvature, r is the curvature radius of the actuator, b_1 and b_2 are the respective width of layer 1 and layer 2, E_1 and E_2 are the respective Young's modulus of layer 1 and layer 2, t_1 and t_2 are the respective length of layer 1 and layer 2, α_1 and α_2 are the respective TEC for layer 1 and layer 2, and ΔT is the temperature variation of the actuator during operation. Here layer 1 is Cu_2O, layer 2 is Cu.

The internal stresses over the cross-section of layer 1 can be divided into a tensile force P_1 and a couple M_1, for layer 2 are a compressive force P_2 and a couple M_2. All forces on the interface must be in equilibrium:

$$P = P_1 = P_2 \quad (2)$$

$$\frac{P(t_1+t_2)}{2} = M_1 + M_2 \quad (3)$$

From beam theory,

$$M_1 = \frac{E_1I_1}{r}, M_2 = \frac{E_2I_2}{r} \quad (4)$$

where I_1 and I_2 is the moment of inertia for layer 1 and layer 2.

In addition, the normal strain of layer 1 and layer 2 must at the interface must be the same, following the equation:

$$\propto_1 \Delta T + \frac{P}{E_1 t_1 b_1} + \frac{t_1}{2r} = \propto_2 \Delta T + \frac{P}{E_2 t_2 b_2} + \frac{t_2}{2r} \tag{5}$$

In our system, due to the porous structure of Cu_2O layer, the apparent CTE of Cu_2O layer is smaller than the dense Cu_2O, so factor (*f*) is introduced to correct the CTE of Cu_2O. And the width of both layers are the same.

By combining and rearranging the terms of (3), (4) and (5), the final expression of curvature can be derived:

$$k = \frac{1}{r} = \frac{6(1+n)^2(\propto_2 - f \propto_1)\Delta T}{h\left[3(1+n)^2 + (1+mn)\left(n^2 + \frac{1}{mn}\right)\right]} \tag{6}$$

$$m = \frac{E_2}{E_1}, n = \frac{t_2}{t_1}, h = t_1 + t_2 \tag{7}$$

Note S5. Temperature of the electric-heating actuator

For a typical situation heated by electric, the temperature of the whole system is balanced between the input electrical power P and the heat loss with environment, as following equation:[2]

$$dT(t) = \frac{\frac{V^2}{R} - (Q_c + Q_r)}{mc} dt \tag{1}$$

where T is the temperature of the heating layer, t is the time, Q_c is the convective power loss, Q_r is the radiative power loss, m is the total mass of the flexible actuator and c is the specific heat capacity. In our system, the power loss is caused through Cu layer and Cu_2O layer. The radiative heat power loss is expressed by the Stefan-Boltzmann law:

$$Q_r = \varepsilon_1 \sigma A_1 (T^4 - T_s^4) + \varepsilon_2 \sigma A_2 (T^4 - T_s^4) \tag{2}$$

where ε_1 and ε_2 are the surface emissivity of Cu layer and Cu_2O layer, σ is the Stefan-Boltzmann constant (5.67 x 10^{-8} $W \cdot m^{-2} \cdot {}^{\circ}C^{-4}$), A_1 and A_2 are the surface area of Cu layer and Cu_2O layer, and T_s is the initial surface temperature. The emissivity of Cu_2O layer is calibrated in Note S2, which is also necessary to measure the temperature accurately. The convective heat power loss is expressed as following:

$$Q_c = h_1 A_1 (T - T_s) + h_2 A_2 (T - T_s) \tag{3}$$

where h_1 and h_2 are the convective heat-transfer coefficient of Cu layer and Cu_2O layer. For a long time of observation, the temperature of the whole system was constant balanced by the heat power loss. Combining and rearranging the equation of (1), (2) and (3), the final equation expresses as following:

$$dT(t) = \frac{1}{mc}\left[\frac{V^2}{R} - h_c A(T(t) - T_s) - \varepsilon\sigma A(T^4(t) - T_s^4)\right]dt \tag{4}$$

$$mc = m_1 c_1 + m_2 c_2 \tag{5}$$

$$h_c = h_1 + h_2 \tag{6}$$

$$\varepsilon = \varepsilon_1 + \varepsilon_2 \tag{7}$$

$$A = A_1 + A_2 \tag{8}$$

where m_1 and m_2 are the mass of Cu layer and Cu_2O layer, c_1 and c_2 are the specific heat capacity of Cu layer and Cu_2O layer, h_c is the total convective heat-transfer coefficient of the actuator, ε is the total surface emissivity of the actuator, and A is the surface area of both Cu layer and Cu_2O layer. The solution of the equation can be expressed as:

$$T(t) = T_s + \frac{V^2}{RhA}(1 - e^{-t/\tau}) \quad \text{with} \quad \tau = \frac{mc}{hA} \tag{9}$$

$$h = h_c + h_r \tag{10}$$

where h_r is the total radiative heat-transfer coefficient of the actuator.

Note S6. Calculation of the bending curvature

The illustration for calculating curvature is shown below. For an actuator with valid actuating length of l, the bending radian θ can be expressed as following:

$$\theta = \frac{l}{r} \tag{1}$$

where r is the radius of curvature for the actuator. Thus the curvature k can be expressed by rearranging the equation (1) with $k = 1/r$:

$$k = \frac{\theta}{l} \tag{2}$$

The bending radian θ is measured by introducing two tangent lines at the beginning and the end of the actuator.

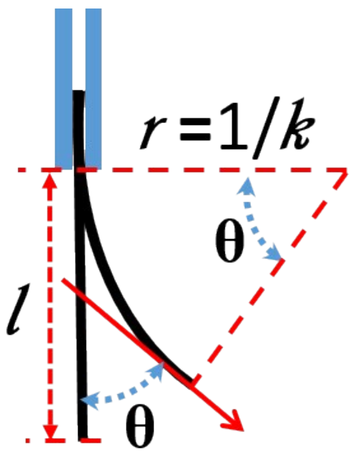

References

[1] S. Timoshenko, *J. Opt. Soc. Am.* 1925, **11**, 233-255.

[2] J.J. Bae, S.C. Lim, G.H. Han, Y.W. Jo, D.L. Doung, E.S. Kim, S.J. Chae, H.Ta Quang, L. Nguyen Van and Y.H. Lee, *Adv. Funct. Mater.* 2012, **22**, 4819-4826.

[3] M. Weng, P. Zhou, L. Chen, L. Zhang, W. Zhang, Z. Huang, C. Liu and S. Fan, *Adv. Funct. Mater.* 2016, **26**, 7244-7253.